Photon-emitter dressed states in a closed waveguide

Davide Lonigro[1,2] Paolo Facchi[1,2] Andrew D. Greentree,[3] Saverio Pascazio[1,2]
Francesco V. Pepe[1,2] and Domenico Pomarico[4]

[1]*Dipartimento di Fisica and MECENAS, Università di Bari, I-70126 Bari, Italy*
[2]*INFN, Sezione di Bari, I-70126 Bari, Italy*
[3]*Australian Research Council Centre of Excellence for Nanoscale Biophotonics,*
School of Science, RMIT University, Melbourne, Victoria 3001, Australia
[4]*Struttura Semplice Dipartimentale di Fisica Sanitaria, I.R.C.C.S. Istituto Tumori "Giovanni Paolo II," I-70124 Bari, Italy*

We study a system made up of one or two two-level quantum emitters, coupled to a single transverse mode of a closed waveguide, in which photon wavenumbers and frequencies are discretized, and characterize the states in which one excitation is steadily shared between the field and the emitters. We unearth finite-size effects in the field-emitter interactions and identify a family of dressed bound states that represent the forerunners of bound states in the continuum in the limit of an infinite waveguide. We finally consider the potential interest of such states for applications in the field of quantum information.

I. INTRODUCTION

One-dimensional and quasi-one-dimensional systems are attracting increasing interest [1], due both to the fundamental and technological relevance of their phenomenology and to the wide range of robust and versatile available experimental platforms, in which dimensional reduction can be efficiently implemented. Among such platforms, it is worth mentioning those based on optical fibers [2,3], cold atoms [4–6], circuit QED [7–13], photonic crystals [14–18], and quantum dots in photonic nanowires [19,20]. In these systems, light propagates in a quasi-one-dimensional geometry with different energy dispersion relations and emitter-photon interaction form factors, determining dimension-dependent features that heavily affect dynamics, decay, and propagation [21,22].

Recent work has been devoted to understand the physics of light-matter coupling in waveguides, systems made up of either single quantum emitters [4,12,23–26] or sets of two [27–41] or even more emitters [17,18,21,23,25,42–61]. In the latter cases, dynamics is deeply influenced by photon-mediated quantum correlations between the emitters, leading to collective phenomena, such as the emergence of superradiant and subradiant states and correlated photon emission. The interplay between distance and wavelength brings to light a number of interesting quantum resonance effects that take place when these two quantities are comparable to each other, thus generalizing the phenomenology observed at very large wavelengths, including Dicke states [62–65].

In this article we characterize the bound states of a system made up of one or two quantum emitters, coupled to a single transverse mode of a closed waveguide. The analysis is performed in the limit in which only the length of the guide is relevant, the other important physical features being independent of its specific geometry. The system we will consider

can be experimentally realized in terms of ring resonators [66,67] or whispering-gallery-mode resonators [68]. Unlike in the case of unbounded waveguides, the system admits an infinite number of bound states, regardless of the features of the coupling. However, their characterization highlights features that are specific to different classes of bound states, which can be identified in many cases as forerunners of the bound and quasibound (unstable) states in an unbounded geometry.

The results are interesting both in view of determining finite-size corrections to the effects identified in the physics of indefinite waveguides, and to identify novel phenomenology that can lead to practical applications. We will indeed show how the properties of a specific class of bound states, related to the wavelength of emitted light resonating with the interatomic distances, suggest the implementation of a qubit in this system.

II. SINGLE EMITTER

A. The model

We first consider one quantum emitter in a closed waveguide of length L, as represented in Fig. 1. In the following analysis, we will assume that effects related to the specific geometry of the waveguide are negligible, though they can play a relevant role in the practical realization of the system.

The emitter is modeled as a two-level system, with its ground $|g\rangle$ and excited $|e\rangle$ states separated by the excitation energy ε, and effectively coupled to a single transverse mode propagating in the waveguide. It is known from waveguide electrodynamics that such a mode behaves as a scalar field with a dispersion relation characterized by an effective photon mass m, inversely proportional to the transverse size of the guide [29,69]. In the case considered here, in which the field
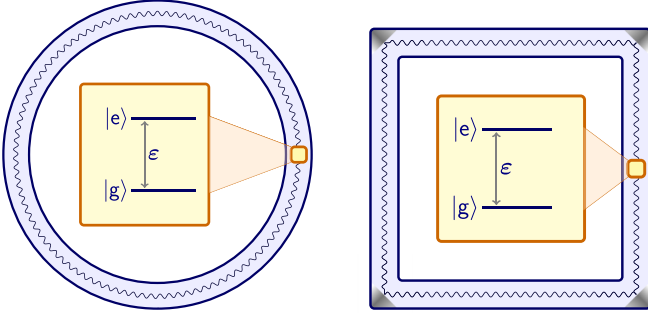
FIG. 1. Single two-level emitter coupled to a transverse mode of a closed waveguide, in a circular (left) and square (right) geometry. In our analysis the specific geometry of the ring is immaterial, only its total length L being relevant.

is also longitudinally confined (and thus subjected to periodic boundary conditions), the allowed photon wavenumbers can take the discrete values $q_k = 2\pi k/L$, with $k \in \mathbb{Z}$, corresponding to the spectrum

$$\omega_k = \sqrt{\left(\frac{2\pi k}{L}\right)^2 + m^2}, \tag{1}$$

where we consider for simplicity a unit system in which the speed of light in the waveguide is $v = 1$. The free part of the Hamiltonian thus reads

$$H_0 = \varepsilon\, \sigma^+\sigma^- + \sum_{k=-\infty}^{\infty} \omega_k b_k^\dagger b_k, \tag{2}$$

where $\sigma^+ = (\sigma^-)^\dagger = |e\rangle\langle g|$ are the atom ladder operators, and b_k the photon longitudinal mode operators, satisfying the canonical commutation relations $[b_k, b_{k'}] = 0$ and $[b_k, b_{k'}^\dagger] = \delta_{kk'}$. The interaction Hamiltonian in the electric dipole atom-field coupling and rotating-wave approximation reads

$$H_{\mathrm{int}} = \sum_{k=-\infty}^{\infty} F_k(\sigma^+ b_k + \sigma^- b_k^\dagger), \tag{3}$$

where the interaction form factor is [29]

$$F_k = \sqrt{\frac{\gamma}{L\omega_k}}, \tag{4}$$

with $\gamma > 0$ being a constant with the dimensions of squared energy. The Hamiltonian model outlined above does not describe photon losses towards external modes, and therefore is able to capture the main features of the dynamics at timescales shorter than the characteristic dissipation times.

The rotating-wave form of the interaction (3) allows diagonalization of the Hamiltonian in sectors with fixed number of excitations $\mathcal{N} = |e\rangle\langle e| + \sum_k b_k^\dagger b_k$. In the $\mathcal{N} = 1$ sector, the state of the system reads

$$|\Psi\rangle = a\,|e\rangle \otimes |\mathrm{vac}\rangle + |g\rangle \otimes \sum_k \xi_k b_k^\dagger |\mathrm{vac}\rangle, \tag{5}$$

where $|\mathrm{vac}\rangle$ is the field vacuum state.

Assume that the atom is placed at $x = 0$; the photon wavefunction $\xi(x)$, with $x \in [-L/2, L/2]$, is given by the Fourier

series

$$\xi(x) = \sqrt{\frac{2\pi}{L}} \sum_k \xi_k e^{\frac{2\pi i k x}{L}}. \tag{6}$$

Normalization adds a further bound on amplitudes:

$$|a|^2 + \int_{-L/2}^{L/2} |\xi(x)|^2\, dx = 1. \tag{7}$$

Notice that the amplitude $\xi(x)$ has dimensions of $L^{-1/2}$, and therefore its squared norm $\int |\xi(x)|^2\, dx$ appearing in the normalization condition is dimensionless as it should be.

B. Atom-photon bound states

We are mainly interested in the eigenstates of the system, in particular those in which the atomic excitation plays a relevant role. We first briefly examine the bound states in the absence of coupling ($\gamma = 0$), and then proceed to the case $\gamma \neq 0$.

1. Bound states in absence of coupling

The free Hamiltonian H_0 admits two types of eigenstates in the one-excitation sector, corresponding to the eigenstates of the two terms in Eq. (2), respectively: (i) excited atom and no photons (i.e., $a = 1$, up to an immaterial global phase), $|\Psi\rangle = |e\rangle \otimes |\mathrm{vac}\rangle$, with energy ε, and (ii) atom in the ground state and a single photon (i.e., $a = 0$), $|\Psi\rangle = |g\rangle \otimes b_k^\dagger |\mathrm{vac}\rangle$, with energy $\omega_k \geqslant m$. In these two cases, for $\varepsilon \neq \omega_k$, the single excitation available to the system is either in the emitter or in the photon field, respectively, since it cannot be exchanged between the two components of the system. As we will see, these two kinds of states (pure-atom and pure-field excitation) correspond to the two limiting cases of atom-photon bound states in the presence of a nonvanishing coupling.

2. Bound states in presence of coupling

When the coupling is switched on, the bound states are modified and the excitation is in general *coherently* shared between atom and field. In order to find them, we must solve the eigenvalue equation for the full Hamiltonian $H = H_0 + H_{\mathrm{int}}$; this is done in Appendix A, where a detailed proof of the following statements is presented. The eigenenergies E are the solutions of the equation

$$E - \varepsilon - \Sigma(E) = 0, \tag{8}$$

where $\Sigma(E)$ is the self-energy function of the atomic excited state [70]:

$$\Sigma(E) = \sum_k \frac{F_k^2}{E - \omega_k}. \tag{9}$$

The amplitudes a and ξ_k in Eq. (5) are determined by the eigenvalue equation and the normalization condition (7):

$$a = [1 - \Sigma'(E)]^{-\frac{1}{2}}, \tag{10}$$

$$\xi_k = \frac{F_k}{E - \omega_k}[1 - \Sigma'(E)]^{-\frac{1}{2}}, \tag{11}$$

where the prime denotes derivative, $\Sigma'(E) = \frac{d\Sigma(E)}{dE}$. As shown in Appendix B, for the form factor (4) one gets the analytic
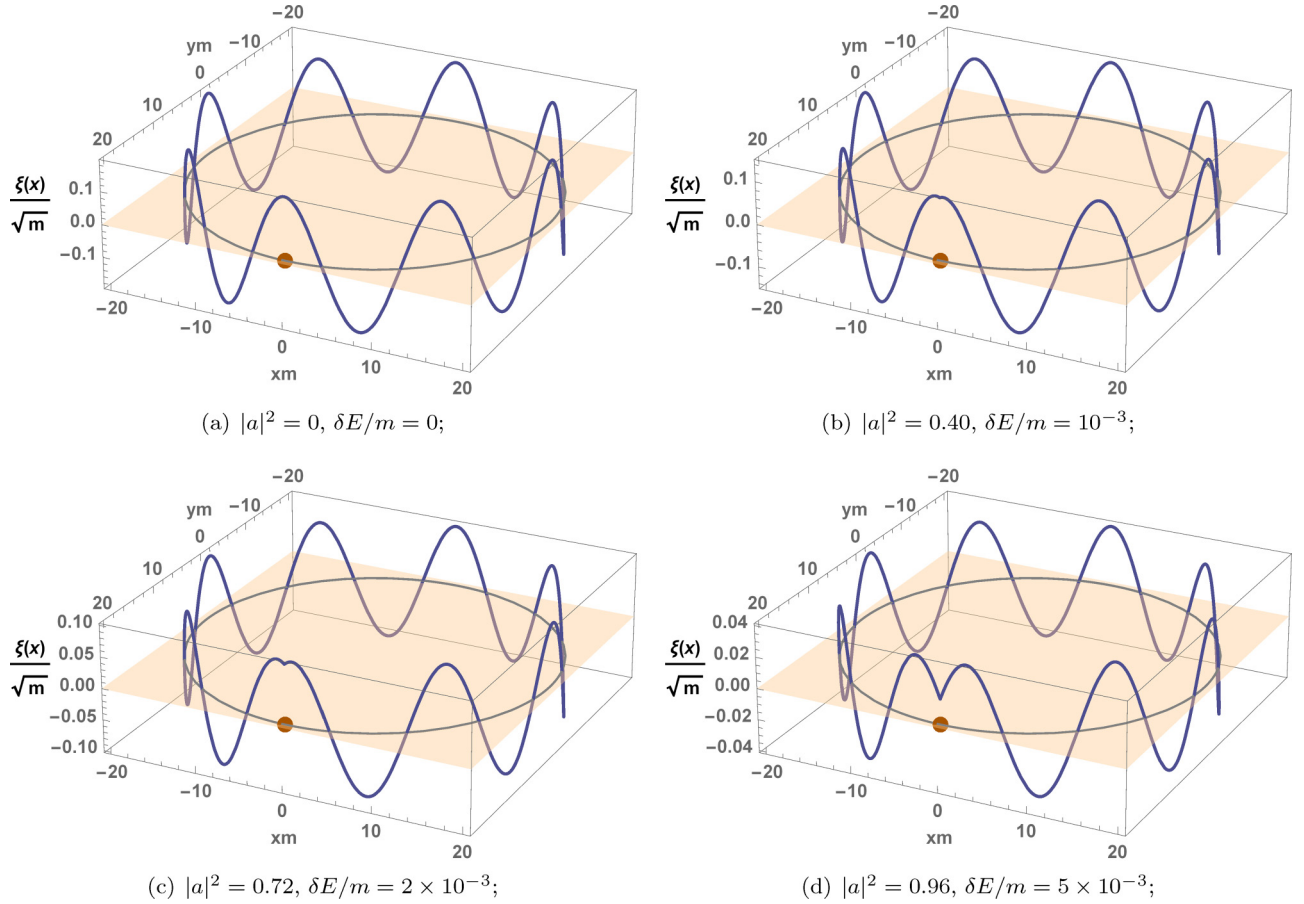
(a) $|a|^2 = 0$, $\delta E/m = 0$;

(b) $|a|^2 = 0.40$, $\delta E/m = 10^{-3}$;

(c) $|a|^2 = 0.72$, $\delta E/m = 2 \times 10^{-3}$;

(d) $|a|^2 = 0.96$, $\delta E/m = 5 \times 10^{-3}$;

FIG. 2. Plots of single-emitter atom-photon bound states with energy $E = \omega_\ell + \delta E$, with $\ell = 8$ and for various values of δE, for the full Hamiltonian $H = H_0 + H_{\text{int}}$ of the system with length $mL = 40\pi$ and coupling $\gamma/m^2 = 10^{-4}$. Each of these bound states is obtained by tuning the excitation energy ε to one of the values given by Eq. (8). (a) The bound state with energy $E \approx \omega_\ell$ with a purely photonic excitation (i.e., $a = 0$); this state coincides with the one obtained in the absence of coupling between the atom and the field: the latter is unaffected by the presence of the atom, and the resulting photon field is smooth at the position $x = 0$ of the emitter. (b), (c) The case of *dressed* bound states with energy $E \neq \omega_\ell$: the atom acquires a nonvanishing portion of excitation, and correspondingly the first derivative of the photon amplitude acquires a discontinuity at $x = 0$. (d) A state with E sufficiently far from any ω_ℓ, in which the atom retains most of the excitation probability. Notice that the z axes of the various figures have different scales: as $|a|^2$ increases, by Eq. (7) the photon field gets smaller. Plotted quantities are dimensionless.

expression

$$\Sigma(E) = \gamma \left(\frac{\cot(q(E)L/2)}{q(E)} \theta(E) + \beta_0(E) \right), \quad (12)$$

with $q(E) = \sqrt{E^2 - m^2}$ and θ being the Heaviside step function. Here $\beta_0(E)$ is a real-valued function bounded by

$$|\beta_0(E)| \leqslant \frac{1}{\pi m} \coth\left(\frac{mL}{2} \right), \quad (13)$$

while the first term in $\Sigma(E)$ diverges at $E = \omega_k$, for all k. Therefore, the eigenvalue equation (8) always admits exactly one solution E_k in each interval (ω_k, ω_{k+1}), so that the eigenvalues alternate with the photon frequencies: $\omega_k < E_k < \omega_{k+1} < E_{k+1}$ (see Fig. 6 in Appendix B).

The photon wavefunction $\xi(x)$, corresponding to an eigenvalue E, is evaluated in Appendix C and reads

$$\xi(x) = a\,\xi_1(x), \quad (14)$$

where

$$\xi_1(x) = \frac{\sqrt{2\pi\gamma E}}{q(E)} [\cot(q(E)L/2) \cos(q(E)x) \\ + \sin(q(E)|x|)]\theta(E) + \eta(x), \quad (15)$$

with $\eta(x)$ being again a small real-valued correction. Examples of photon wavefunctions are reported in Fig. 2.

Having solved explicitly the eigenproblem for our system, we can discuss the properties of the eigenenergies and the corresponding bound states for different values of the parameters. If $\omega_\ell < \varepsilon < \omega_{\ell+1}$, we can outline the following typical features of the eigenstates in the perturbative regime: eigenvalues $E_k \neq E_\ell$ correspond to states that are generally dominated by a symmetric combination of photon excitations with opposite momenta, whose energy is, respectively, slightly smaller than ω_{k+1} (for $E_k < E_\ell$) or slightly larger than ω_k (for $E_k > E_\ell$); the eigenvalue E_ℓ is close to ε, up to a correction of $O(\gamma)$, and corresponds to a state with a dominant atomic excitation. A value of ε very close to a photon frequency ω_ℓ generates two
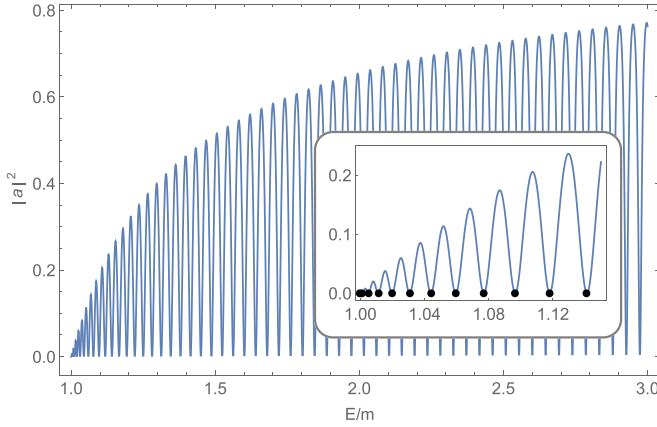
FIG. 3. Emitter excitation probability $|a|^2$, given by Eq. (10), in an eigenstate with energy E, for $mL = 40\pi$ and $\gamma/m^2 = 10^{-4}$. The probability that the emitter is in its excited state vanishes at the photon frequencies ω_k, with $k \in \mathbb{Z}$: the corresponding states are the same that would be obtained in the absence of the emitter. Values of E for which $|a|^2$ is nonzero correspond to bound states in which the emitter shares part of the excitation. For these states, the derivative of the photon field acquires a discontinuity at the position of the emitter, and the norm of the photon wavefunction decreases (see Fig. 2). Plotted quantities are dimensionless.

eigenstates, with energies above and below ω_ℓ, in which the photon and the atomic excitation are strongly hybridized. By increasing γ, the eigenvalues E_k migrate towards the center of the intervals (ω_k, ω_{k+1}), indicating a stronger superposition between atomic and photonic excitations, with a significant involvement of photons with different wavenumbers. Notice that, in any regime, the parameters can be tuned to select a given value of the emitter excitation probability, as summarized in Fig. 3.

Finally, it is interesting to study what happens in the limit of a large ring. By increasing the value of L, energy eigenvalues become more and more dense, and the value $|a|^2$ of the atomic excitation probability decreases. In a semiclassical picture, for $L \to \infty$ the photon emitted by the atom will take an infinite time to return to the emitter, which will have released a larger part of its excitation in the meanwhile. None of the eigenstates survives the limit $L \to \infty$: this is expected, since the system becomes locally equivalent to an infinite-length linear waveguide, in which no bound state with energy $E > m$ emerges, for a nonvanishing form factor, in the single-emitter case, though bound excited states of two or more emitters are possible [29].

III. TWO EMITTERS

We now consider the case in which two identical emitters, with equal excitation energy ε and positions x_1 and x_2 at a distance d, are coupled to a transverse waveguide mode. Their ground and excited states will be denoted by $|g_\alpha\rangle$ and $|e_\alpha\rangle$, with $\alpha = 1, 2$, respectively. The two emitters interact with each other only by photon exchange, and no direct coupling is assumed. The interaction Hamiltonian, which generalizes

Eq. (3), reads

$$H_{\text{int}} = \sum_{k=-\infty}^{\infty} \sum_{\alpha=1,2} F_k \big(e^{\frac{2\pi i k x_\alpha}{L}} \sigma_\alpha^+ b_k + e^{\frac{-2\pi i k x_\alpha}{L}} \sigma_\alpha^- b_k^\dagger \big), \quad (16)$$

and the state in the one-excitation sector is

$$|\Psi\rangle = \sum_{\alpha=1,2} a_\alpha \sigma_\alpha^+ |G\rangle \otimes |\text{vac}\rangle + |G\rangle \otimes \sum_k \xi_k b_k^\dagger |\text{vac}\rangle, \quad (17)$$

with $|G\rangle = |g_1\rangle \otimes |g_2\rangle$.

A. Bound states

As in the single-emitter case, in order to evaluate the bound states of the system we must solve the eigenproblem; this is done in Appendix C, where we prove the following statements. The eigenvalue E corresponding to an eigenstate with finite atomic excitation amplitude obeys the equation

$$\det\left[(E - \varepsilon)\mathbb{1} - \Sigma(E)\right] = 0, \quad (18)$$

where the self-energy is now a 2×2 matrix, and $\mathbb{1}$ is the identity matrix. The atom amplitude vector $\boldsymbol{a} = (a_1, a_2)^T$ characterizing the corresponding eigenstate satisfies

$$\left[(E - \varepsilon)\mathbb{1} - \Sigma(E)\right]\boldsymbol{a} = 0, \quad (19)$$

which fixes a_1 and a_2 up to a global multiplication constant (notice that, generally, $\|\boldsymbol{a}\| < 1$), while the photon amplitudes are determined by a straightforward generalization of Eq. (11). The values of a_j and ξ_k are eventually fixed, up to an overall phase factor, by state normalization. Also in this case, one can derive an analytical form of the self-energy,

$$\Sigma_{j\ell}(E) = \frac{\gamma}{q(E)} A_{j\ell}(q(E))\theta(E) + \gamma \beta_{j-\ell}(E), \quad (20)$$

where $q(E) = \sqrt{E^2 - m^2}$,

$$A_{j\ell}(q) = \cot\left(\frac{qL}{2}\right) \cos\left((j-\ell)qd\right) + \sin\left(|j-\ell|qd\right), \quad (21)$$

β_0 is the same function that appears in Eq. (12), and $\beta_1 = \beta_{-1}$ is a function suppressed like $|\beta_1(E)| \leqslant [e^{-m(L-d)} + e^{-md}]/(\pi m)$. By neglecting the latter contribution for $md, m(L-d) \gg 1$, the energies of the bound states are determined by the solutions of the following equations:

$$E \simeq \varepsilon + \frac{\gamma}{q(E)} \chi^{(n)}(q(E)) + \gamma \beta_0(E), \quad (22)$$

where $\chi^{(n)}(q)$, with $n = 1, 2$, are the eigenvalues, possibly coincident, of the matrix $A(q)$. As in the single-emitter case, the right-hand side diverges at each ω_k, providing a set of energy pairs $\{E_k^{(1)}, E_k^{(2)}\}$ in each interval (ω_k, ω_{k+1}). The corresponding value of the ratio a_2/a_1 is determined by the eigenvector of A corresponding to the specific eigenvalue $\chi^{(n)}$.

Correspondingly, the photon wavefunction will be

$$\xi(x) = a_1 \xi_1(x - x_1) + a_2 \xi_1(x - x_2), \quad (23)$$

with $\xi_1(x)$ as in Eq. (15), and $-L/2 \leqslant x_1 < x_2 < L/2$ being the positions of the two emitters. An analogous result holds when more than two emitters are considered.

B. A special case: Resonant states

As in the single-emitter case, the bound state energy can take any value $E > m$ depending on ε, γ, and m. Instead of discussing the eigenproblem for the two-emitter system in the general case, we focus on a case of particular interest, which is a forerunner of effects observed in an infinite waveguide. Namely, we study the eigenvalues that *resonate* with the distance d between the emitters, that is,

$$E = E_\nu = \sqrt{\left(\frac{\nu\pi}{d}\right)^2 + m^2}, \quad \nu = 1, 2, \ldots, \quad (24)$$

for which an integer number of half wavelengths $\pi/q(E_\nu) = d/\nu$ [generally not coinciding with any of the half wavelengths $\pi/q_k = L/(2k)$ of the photon in the ring] separate the two emitters. We refer to this particular class of bound states as *resonant states*.

For this class of bound states, the atomic excitation is determined, up to $O(e^{-md})$, by the eigenstates of the matrix

$$A\left(\frac{\nu\pi}{d}\right) = \cot\left(\frac{\pi\nu L}{2d}\right)\begin{pmatrix} 1 & (-1)^\nu \\ (-1)^\nu & 1 \end{pmatrix}. \quad (25)$$

The eigenvalues are $\chi^{(1)} = 0$, corresponding to a solution with $a_2/a_1 = (-1)^{\nu+1}$, occurring for values of atomic excitation energy satisfying $\varepsilon = E_\nu + \beta_0(E_\nu)$, and $\chi^{(2)} = 2\cot(\pi\nu L/2d)$, related to an eigenstate with opposite atomic excitation parity, $a_2/a_1 = (-1)^\nu$, occurring when

$$\varepsilon = E_\nu + \beta_0(E_\nu) - 2\gamma d \cot(\pi\nu L/2d)/(\nu\pi). \quad (26)$$

It is evident that, while the former energy eigenvalue is practically independent of L, the latter wildly oscillates as L increases. Indeed, one of the states converges to a true bound state on the infinite waveguide, in which the atomic excitations are combined in such a way to confine the field between the emitter, while the orthogonal combination becomes part of an unbound state, characterized by twice the decay rate of an isolated atom [29].

Such states have the following peculiar property: the photon wavefunction corresponding to a resonant state is *confined*, up to a small correction, in the region of space between the two atoms. Indeed, by Eqs. (15)–(23), and by noticing that, as a consequence of Eq. (24), $q(E_\nu) = \nu\pi/d$, by setting the positions of the two atoms at $x = 0$ and $x = d$ and discarding the contributions of the terms $\eta(x)$ and $\eta(x - d)$ coming from Eq. (15), we have

$$\xi(x) = \begin{cases} \sqrt{\frac{2\pi\gamma E_\nu d}{\nu\pi}} \sin\left(\frac{\nu\pi x}{d}\right), & 0 \leqslant x \leqslant d \\ 0, & \text{otherwise.} \end{cases} \quad (27)$$

In particular, both atoms are placed at nodes of the photon wavefunction. Interestingly, there is no dependence on L in the previous equation; in particular, these states survive the limit $L \to \infty$, where bound states in the continuum (BIC) [71] are expected to emerge [29]. On the contrary, nonresonant (and thus not confined) bound states generally *do depend* on L and do not survive in the limit, merging in the continuum of scattering (non-normalized) states. We remark that resonant bound states are robust with respect to small variations in
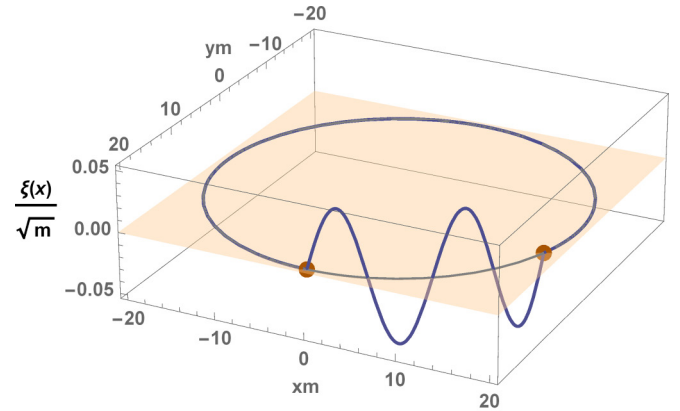
(a) $a_1 + a_2 = 0$, $|a_1|^2 + |a_2|^2 = 0.966$, $E = E_4$
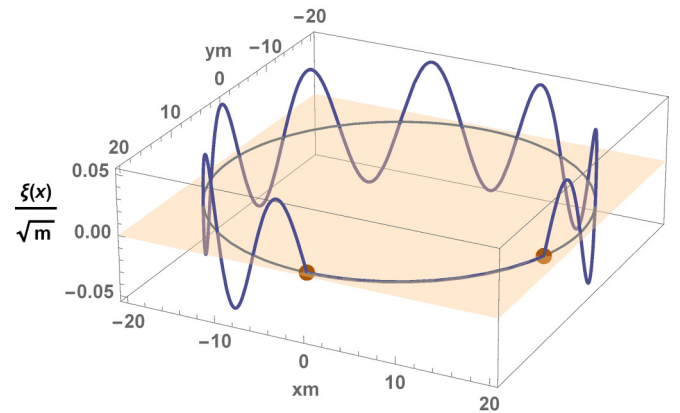
(b) $a_1 - a_2 = 0$, $|a_1|^2 + |a_2|^2 = 0.934$, $E = \tilde{E}_{15}$

FIG. 4. Photon amplitudes in two resonant bound states occurring in the same system. An integer number of half wavelengths, corresponding to approximately the same energy, can be accommodated in the shortest (of length d) and longest (of length $L - d$) path connecting the two emitters. We set $mL = 40\pi$, $md = 25$, and $\gamma/m^2 = 10^{-4}$. Plotted quantities are dimensionless.

the interatomic distance, in the $L \to \infty$ limit, as shown in Ref. [29].

Given the value d of the distance, a complementary set of resonant bound states exists, besides the ones discussed above, corresponding to the energies

$$E = \tilde{E}_\nu = \sqrt{\left(\frac{\nu\pi}{L - d}\right)^2 + m^2}, \quad \nu = 1, 2, \ldots. \quad (28)$$

These states are characterized by the fact that the region between the emitters, of length $L - d$, is [up to $O(e^{-md})$] a multiple of the half wavelength associated with the eigenvalue. Their properties are obtained by merely replacing d with $L - d$ in the above equations. However, none of these eigenstates survives as a bound state in the $L \to \infty$ limit.

IV. APPLICATIONS

An interesting situation occurs in the case, depicted in Fig. 4, when the energy E_ν of a resonant state with non-vanishing field in the inner region between the emitters approximately coincides with the energy $\tilde{E}_{\nu'}$ of a resonant

state with the field confined in the outer region of length $L - d$ and with opposite atomic parity, for some pair (ν, ν') of integers. Clearly, this case can occur only when d and $L - d$ are at least approximately commensurable. The relevance of this case lies in the fact that these two states, quasidegenerate and orthogonal to each other, represent the pair $\{E_k^{(1)}, E_k^{(2)}\}$ of eigenvalues expected in some interval (ω_k, ω_{k+1}), and are therefore separated from the other eigenvalues by a quantity $\sim L^{-1}$. Thus, especially for small waveguide lengths, the energy separation of the complementary resonant states allows them to be coherently addressed and manipulated as a two-level system, provided the energy scale g of the external coupling satisfies

$$g \ll |E_\nu - \omega_{\bar{k}}|, \tag{29}$$

with $\bar{k}$ the closest integer to $\nu L/2d$. In this case, the subspace spanned by the two resonant states is a good candidate for a robust qubit, and coherent manipulation can occur by applying an external driving field (either time dependent or time independent, according to the performed tasks) to one or both emitters, while measurement in the computational basis can be performed by detecting the photon in the inner or outer region.

Finally, it is worth addressing the nontrivial task of reading the emitter state. The challenge arising in this field reflects the tension between the need for the system to be closed for free dynamics and open for readout, and for the latter to be performed without damaging the properties of the isolated system. A possible strategy to extract information on the state of the emitters can consist in the coupling with modes that leak into the waveguide from the outer space [72], that is negligible during dynamics, but could be enhanced by either enacting a Q-switching process [73], bringing in another waveguide into the evanescent mode, or by properly tuning in and out of resonance the relevant optical parameters. The last technique is applied, for example, in Ref. [10], by tuning the atomic excitation frequency out of resonance with the external field for the duration of the measurement.

V. CONCLUSIONS

We have outlined the features of bound states in systems of one and two emitters coupled to a single transverse mode of a closed linear waveguide. In these eigenstates, the atomic and photonic excitations are dressed by interaction and hybridized with each other. In the two-emitter case, we have unearthed the existence of pairs of quasidegenerate eigenstates, that represent the forerunners of the bound states in the continuum observed in unbounded geometries. Such a feature, which is absent in unbounded waveguides, opens the possibility to implement a qubit. A promising experimental platform to realize the described system is represented by superconducting qubits coupled to transmission line resonators [74,75], as well as in one-dimensional slot waveguide and related types of structures [76], that can be used to implement configurations analogous to the one in the right-hand panel of Fig. 1.

Future research will focus on specific entangled states in multiemitter configurations and on the analysis of moving emitters [77], in which the interplay between internal and translational degrees of freedom can yield interesting effects.

APPENDIX A: EIGENVALUE EQUATION

1. One emitter

The state in the one-excitation sector has the form given in Eq. (5):

$$|\Psi\rangle = a\,|e\rangle \otimes |\text{vac}\rangle + |g\rangle \otimes \sum_k \xi_k b_k^\dagger |\text{vac}\rangle$$

$$= a\,|e, \text{vac}\rangle + \sum_k \xi_k\,|g, k\rangle, \tag{A1}$$

and the action of the Hamiltonian $H = H_0 + H_{\text{int}}$, given in Eqs. (2) and (3), on the basis vectors reads

$$H\,|e, \text{vac}\rangle = \varepsilon\,|e, \text{vac}\rangle + \sum_k F_k\,|g, k\rangle,$$

$$H\,|g, k\rangle = \omega_k\,|g, k\rangle + F_k\,|e, \text{vac}\rangle. \tag{A2}$$

Therefore, the eigenvalue equation $H\,|\Psi\rangle = E\,|\Psi\rangle$ projected on the basis vectors gives

$$(E - \varepsilon)a + \sum_k F_k \xi_k = 0,$$

$$(E - \omega_k)\xi_k + F_k a = 0. \tag{A3}$$

By solving the second equation,

$$\xi_k = \frac{F_k}{E - \omega_k}a, \tag{A4}$$

and plugging it into the first one, we finally get

$$(E - \varepsilon - \Sigma(E))a = 0, \tag{A5}$$

where

$$\Sigma(E) = \sum_k \frac{F_k^2}{E - \omega_k} \tag{A6}$$

is the self-energy function of the model. This gives Eq. (8). The state normalization $|a|^2 + \sum_k |\xi_k|^2 = 1$ gives

$$|a|^2\left(1 + \sum_k \frac{F_k^2}{(E - \omega_k)^2}\right) = |a|^2\left(1 - \frac{d}{dE}\Sigma(E)\right) = 1, \tag{A7}$$

from which we get Eqs. (10) and (11).

2. Two emitters

The computation is a straightforward generalization of the one-emitter case. The state in the one-excitation sector has the

form given in Eq. (17):

$$|\Psi\rangle = \sum_{\alpha=1,2} a_\alpha \sigma_\alpha^+ |G\rangle \otimes |\text{vac}\rangle + |G\rangle \otimes \sum_k \xi_k b_k^\dagger |\text{vac}\rangle$$

$$= a_1 |e_1, \text{vac}\rangle + a_2 |e_2, \text{vac}\rangle + \sum_k \xi_k |G, k\rangle, \qquad (A8)$$

and the action of the Hamiltonian $H = H_0 + H_{\text{int}}$ on the basis vectors reads

$$H |e_1, \text{vac}\rangle = \varepsilon |e_1, \text{vac}\rangle + \sum_k F_k e^{\frac{-2\pi i k x_1}{L}} |G, k\rangle,$$

$$H |e_2, \text{vac}\rangle = \varepsilon |e_2, \text{vac}\rangle + \sum_k F_k e^{\frac{-2\pi i k x_2}{L}} |G, k\rangle,$$

$$H |G, k\rangle = \omega_k |G, k\rangle + F_k e^{\frac{2\pi i k x_1}{L}} |e_1, \text{vac}\rangle$$
$$+ F_k e^{\frac{2\pi i k x_2}{L}} |e_1, \text{vac}\rangle. \qquad (A9)$$

Therefore, the eigenvalue equation $H |\Psi\rangle = E |\Psi\rangle$ projected on the basis vectors gives

$$(E - \varepsilon)a_1 + \sum_k F_k e^{\frac{2\pi i k x_1}{L}} \xi_k = 0,$$

$$(E - \varepsilon)a_2 + \sum_k F_k e^{\frac{2\pi i k x_2}{L}} \xi_k = 0, \qquad (A10)$$

$$(E - \omega_k)\xi_k + F_k e^{\frac{-2\pi i k x_1}{L}} a_1 + F_k e^{\frac{-2\pi i k x_2}{L}} a_2 = 0.$$

By solving the third equation,

$$\xi_k = \frac{F_k}{E - \omega_k}\left(e^{\frac{-2\pi i k x_1}{L}} a_1 + e^{\frac{-2\pi i k x_2}{L}} a_2 \right), \qquad (A11)$$

and plugging it into the first and the second one, we finally get

$$[(E - \varepsilon)\mathbb{1} - \Sigma(E)]\boldsymbol{a} = 0, \qquad (A12)$$

where $\boldsymbol{a} = (a_1, a_2)^T$, and $\Sigma(E) = (\Sigma_{j\ell}(E))_{j,\ell=1,2}$, with

$$\Sigma_{j\ell}(E) = \sum_k \frac{F_k^2}{E - \omega_k} e^{\frac{2\pi i k(x_j - x_\ell)}{L}}, \qquad (A13)$$

which is the 2×2 self-energy matrix of the model. This gives Eq. (20). The energy of the nontrivial solution must satisfy

$$\det[(E - \varepsilon)\mathbb{1} - \Sigma(E)] = 0, \qquad (A14)$$

that is Eq. (18).

APPENDIX B: CALCULATION OF THE SELF-ENERGY

The self-energy of the model has matrix elements given by

$$\Sigma_{j\ell}(E) = \sum_k \frac{F_k^2}{E - \omega_k} \exp\left(\frac{2\pi i k(x_j - x_\ell)}{L} \right)$$
$$= \frac{\gamma}{L} \sum_{k=-\infty}^\infty \frac{1}{\omega_k(E - \omega_k)} \exp\left(\frac{2\pi i k(x_j - x_\ell)}{L} \right), \qquad (B1)$$

where

$$\omega_k = \sqrt{\left(\frac{2\pi k}{L} \right)^2 + m^2} \qquad (B2)$$
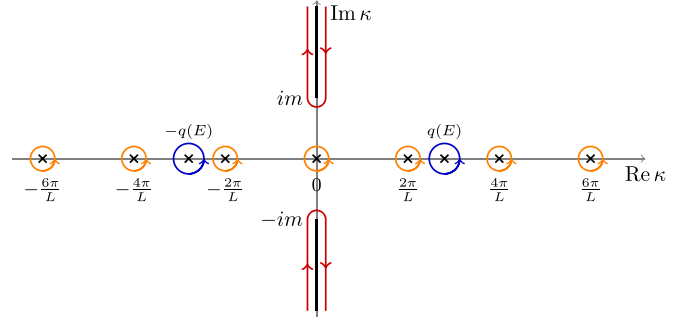

FIG. 5. Integration contour of the complex function $f_{E,d}(\kappa)$ in the complex plane. The integral over the path Γ (the two red curves), here chosen in such a way to encircle the two branch cuts of the function, equals the sum of its residua, namely, those corresponding to the points $\kappa = \frac{2\pi k}{L}$, $k \in \mathbb{Z}$ (orange small circles), plus the ones corresponding to the points $\kappa = \pm q(E)$, $q(E) = \sqrt{E^2 - m^2}$, as far as $E > 0$ (blue large circles).

and x_j, x_ℓ are the positions of the emitters in the guide. The diagonal elements $\Sigma_{11}(E) = \Sigma_{22}(E)$ are nothing but the single-emitter self-energy function discussed in Sec. II. Notice that, because of the property $\omega_{-k} = \omega_k$, $\Sigma_{j\ell}(E) = \Sigma_{\ell j}(E)$; therefore, we can equivalently write

$$\Sigma_{j\ell}(E) = \frac{\gamma}{L} \sum_{k=-\infty}^\infty \frac{1}{\omega_k(E - \omega_k)} \exp\left(\frac{2\pi i k d_{j\ell}}{L} \right), \qquad (B3)$$

with $d_{j\ell} = |x_j - x_\ell|$. Also notice that the self-energy is invariant under the transformation

$$d_{j\ell} \to L - d_{j\ell}, \qquad (B4)$$

as it must be since the physics of the system cannot depend on the orientation of the coordinate system.

To compute $\Sigma_{j\ell}(E)$ we will make use of the "Herglotz trick" of the cotangent, a beautiful argument which allows to determine the series by a complex integration [78]. Consider the following function on the complex κ plane:

$$f_{E,d}(\kappa) = \frac{e^{id\kappa}}{\sqrt{\kappa^2 + m^2}(E - \sqrt{\kappa^2 + m^2})} \pi \left[\cot\left(\frac{\kappa L}{2} \right) - i \right], \qquad (B5)$$

the complex square root to be interpreted in the sense of the principal value; we will fix $0 < d < L$. For every real E, this is a meromorphic function in $\mathbb{C} \setminus [\pm im, \pm i\infty)$ having (a) simple poles at $\kappa = \frac{2k\pi}{L}$ for all $k \in \mathbb{Z}$; (b) two simple poles at $\kappa = \pm q(E) = \pm\sqrt{E^2 - m^2}$, as far as $E > 0$; and (c) two branch cuts along $\pm i[m, \infty)$. Besides, it is exponentially bounded at ∞ in both half planes: indeed, one gets

$$e^{id\kappa}\left[\cot\left(\frac{\kappa L}{2} \right) - i \right] = 2i \frac{e^{id\kappa}}{e^{iL\kappa} - 1}, \qquad (B6)$$

where its modulus for $\kappa = iy$, $y > 0$, decays as e^{-dy}, while for $\kappa = -iy$, $y > 0$, it decays as $e^{-(L-d)y}$.

By the residue theorem, the integral of $f_{E,d}(\kappa)$ on any positively oriented contour Γ (see Fig. 5) which includes all

its simple poles is given by

$$
\frac{1}{2\pi i} \oint_{\Gamma} f_{E,d}(\kappa)\, d\kappa
$$

$$
= \sum_{k=-\infty}^{\infty} \mathrm{Res}_{f_{E,d}}\left(\frac{2\pi k}{L}\right) + \mathrm{Res}_{f_{E,d}}(\sqrt{E^2-m^2})\theta(E)
$$

$$
+ \mathrm{Res}_{f_{E,d}}(-\sqrt{E^2-m^2})\theta(E), \qquad (B7)
$$

where $\theta(E)$ is the Heaviside step function. An immediate calculation shows that

$$
\mathrm{Res}_{f_{E,d}}\left(\frac{2\pi k}{L}\right) = \frac{2\pi}{L}\frac{1}{\omega_k(E-\omega_k)}\exp\left(\frac{2\pi i k d}{L}\right), \quad (B8)
$$

while

$$
\mathrm{Res}_{f_{E,d}}(\pm\sqrt{E^2-m^2})
$$

$$
= -\frac{\mathrm{e}^{\pm i d \sqrt{E^2-m^2}}}{\sqrt{E^2-m^2}}\pi\left[\cot\left(\frac{L\sqrt{E^2-m^2}}{2}\right)\mp i\right], \quad (B9)
$$

implying that

$$
\frac{2\pi}{L}\sum_{k=-\infty}^{\infty}\frac{1}{\omega_k(\omega_k-E)}\exp\left(\frac{2\pi i k d}{L}\right) = 2\pi\frac{\cot\left(\frac{L\sqrt{E^2-m^2}}{2}\right)\cos(d\sqrt{E^2-m^2})+\sin(d\sqrt{E^2-m^2})}{\sqrt{E^2-m^2}}\theta(E) + \frac{1}{2\pi i}\oint_{\Gamma} f_{E,d}(\kappa)\, d\kappa.
$$

$$
(B10)
$$

Let us focus on the integral along the integration contour Γ; while the choice of Γ is immaterial, it will be convenient to choose a contour which encircles both branch cuts of $f_{E,d}(\kappa)$ as in Fig. 5; that is,

$$
\oint_{\Gamma} f_{E,d}(\kappa)\, d\kappa = \int_{im-0^+}^{i\infty-0^+} f_{E,d}(\kappa)\, d\kappa - \int_{im+0^+}^{i\infty+0^+} f_{E,d}(\kappa)\, d\kappa + \int_{-im+0^+}^{-i\infty+0^+} f_{E,d}(\kappa)\, d\kappa - \int_{-im-0^+}^{-i\infty-0^+} f_{E,d}(\kappa)\, d\kappa
$$

$$
= i\int_m^\infty (f_{E,d}(iy-0^+)-f_{E,d}(iy+0^+))\, dy - i\int_m^\infty (f_{E,d}(-iy+0^+)-f_{E,d}(-iy-0^+))\, dy
$$

$$
= -2\pi i\int_m^\infty \frac{\mathrm{e}^{-dy}}{\mathrm{e}^{-Ly}-1}\frac{1}{\sqrt{y^2-m^2}}\frac{2E}{E^2+y^2-m^2}\, dy + 2\pi i\int_m^\infty \frac{\mathrm{e}^{dy}}{\mathrm{e}^{Ly}-1}\frac{1}{\sqrt{y^2-m^2}}\frac{2E}{E^2+y^2-m^2}\, dy
$$

$$
= 4\pi i\int_m^\infty \frac{\mathrm{e}^{-dy}+\mathrm{e}^{-(L-d)y}}{1-\mathrm{e}^{-Ly}}\frac{1}{\sqrt{y^2-m^2}}\frac{E}{E^2+y^2-m^2}\, dy
$$

$$
= 4\pi i\int_m^\infty \frac{\cosh(dy)\coth\left(\frac{Ly}{2}\right)-\sinh(dy)}{\sqrt{y^2-m^2}}\frac{E}{E^2+y^2-m^2}\, dy. \qquad (B11)
$$

Notice that the latter contribution is invariant under the transformation $d \to L-d$. We finally get

$$
\Sigma_{j\ell}(E) = \gamma\frac{\cot\left(\frac{L\sqrt{E^2-m^2}}{2}\right)\cos(d_{j\ell}\sqrt{E^2-m^2})+\sin(d_{j\ell}\sqrt{E^2-m^2})}{\sqrt{E^2-m^2}}\theta(E) + \gamma\beta_{j-\ell}(E), \qquad (B12)
$$

where the functions

$$
\beta_{j-\ell}(E) = \frac{1}{\pi}\int_m^\infty \frac{\cosh(d_{j\ell}y)\coth\left(\frac{Ly}{2}\right)-\sinh(d_{j\ell}y)}{\sqrt{y^2-m^2}}\frac{E}{E^2+y^2-m^2}\, dy \qquad (B13)
$$

appear in Eq. (20). In particular, for $j=\ell$, one gets $d_{j\ell}=0$ and the above expressions reduce to the single-emitter case:

$$
\Sigma(E) = \gamma\frac{\cot\left(\frac{L\sqrt{E^2-m^2}}{2}\right)}{\sqrt{E^2-m^2}}\theta(E) + \gamma\beta_0(E), \qquad (B14)
$$

with

$$
\beta_0(E) = \frac{1}{\pi}\int_m^\infty \frac{\coth\left(\frac{Ly}{2}\right)}{\sqrt{y^2-m^2}}\frac{E}{E^2+y^2-m^2}\, dy. \qquad (B15)
$$

This is the expression whose upper bound is shown in Eq. (13).

Consider energies $E \geqslant 0$. As long as $d < L$, the integrand in Eq. (B13) is a positive, monotonically decreasing function of y, since

$$
\frac{d}{dy}\frac{\mathrm{e}^{-d_{j\ell}y}-\mathrm{e}^{-(L-d_{j\ell})y}}{1-\mathrm{e}^{-Ly}} = -\frac{1}{2}[(L-d_{j\ell})\cosh(d_{j\ell}y)+d_{j\ell}\cosh((L-d_{j\ell})y)]\,\mathrm{csch}\left(\frac{Ly}{2}\right)^2. \qquad (B16)
$$

Consequently, we have

$$\beta_{j\ell}(E) \leqslant \frac{1}{\pi}\left[\cosh(md_{j\ell})\coth\left(\frac{mL}{2}\right) - \sinh(md_{j\ell})\right]\int_m^\infty \frac{1}{\sqrt{y^2-m^2}}\frac{E}{E^2+y^2-m^2}\,dy$$

$$= \frac{1}{\pi}\left[\cosh(md_{j\ell})\coth\left(\frac{mL}{2}\right) - \sinh(md_{j\ell})\right]\frac{\text{arcsinh}\left(\frac{\sqrt{E^2-m^2}}{m}\right)}{\sqrt{E^2-m^2}}$$

$$= \frac{1}{\pi}\left[\frac{e^{-m(L-d_{j\ell})}+e^{-md_{j\ell}}}{1-e^{-mL}}\right]\frac{\text{arcsinh}\left(\frac{\sqrt{E^2-m^2}}{m}\right)}{\sqrt{E^2-m^2}}. \tag{B17}$$

In particular,

$$\beta_0(E) \leqslant \frac{1}{\pi}\coth\left(\frac{mL}{2}\right)\frac{\text{arcsinh}\left(\frac{\sqrt{E^2-m^2}}{m}\right)}{\sqrt{E^2-m^2}}$$

$$\leqslant \frac{1}{\pi m}\coth\left(\frac{mL}{2}\right) \tag{B18}$$

is positive and bounded for all positive energies. Moreover, if *both* $md \gg 1$ and $m(L-d) \gg 1$, i.e., the two emitters are sufficiently far away, $\beta_1(E) = \beta_{-1}(E)$ will be small and may be neglected:

$$|\beta_1(E)| = |\beta_{-1}(E)| \leqslant \frac{1}{\pi m}[e^{-m(L-d)}+e^{-md}]. \tag{B19}$$

Mathematically, the contribution of the upper and lower parts of the contour in Fig. 5 yield, respectively, an $O(e^{-md})$ and an $O(e^{-m(L-d)})$ contribution to $\Sigma_{12}(E)$.

Having computed the self-energy, in principle we can solve the eigenvalue problem for the model. In particular, in Fig. 6 we provide a graphical analysis of the solutions of the eigenvalue equation (A5) for the single emitter in a waveguide for a suitable choice of the parameters; we have countably many eigenvalues above the mass threshold $E > m$, each being em-
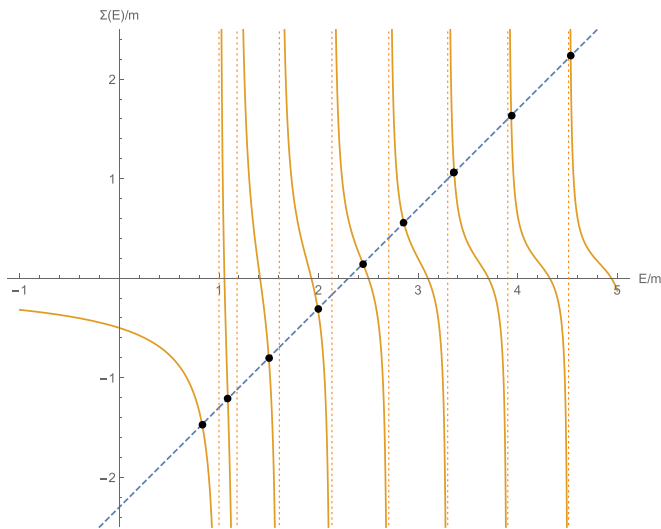

FIG. 6. Solutions of Eq. (A5) with $\varepsilon/m = 2.3$ and $mL = 10$. The orange solid curve corresponds to the self-energy, its asymptotes, represented as orange dotted vertical lines, corresponding to the values ω_k, $k = 0, \pm1, \pm2, \ldots$, in Eq. (B2); the dashed blue line is the graph of $E - \varepsilon$. The abscissa of each black dot is a solution of the eigenvalue equation. Plotted quantities are dimensionless.

bedded between two consecutive eigenenergies ω_k, ω_{k+1} of the uncoupled system. In particular, eigenvalues far from ε will be close to the extrema of the interval (ω_k, ω_{k+1}), regardless of the choice of the parameters, while eigenvalues close to ε will lie somewhere in the middle and will be sensibly dependent on the parameters. Notice that the model will also exhibit a single eigenvalue below m, corresponding to an evanescent boson field concentrated around the emitter.

APPENDIX C: PHOTON WAVEFUNCTION

Let us finally evaluate the photon wavefunction associated with a bound state of the system. Recalling our discussion in Appendix A, respectively in the single-emitter case, Eq. (A4), and in the two-emitter case, Eq. (A11), we have, up to an overall normalization constant,

$$\xi(x) = a\,\xi_1(x), \tag{C1}$$

$$\xi(x) = a_1\xi(x-x_1) + a_2\xi_1(x-x_2), \tag{C2}$$

where, in both cases,

$$\xi_1(x) = \frac{\sqrt{2\pi\gamma}}{L}\sum_{k=-\infty}^{\infty}\frac{1}{\sqrt{\omega_k}(E-\omega_k)}\exp\left(\frac{2\pi ikx}{L}\right). \tag{C3}$$

Since $\omega_{-k} = \omega_k$, we can equivalently write

$$\xi_1(x) = \frac{\sqrt{2\pi\gamma}}{L}\sum_{k=-\infty}^{\infty}\frac{1}{\sqrt{\omega_k}(E-\omega_k)}\exp\left(\frac{2\pi ik|x|}{L}\right). \tag{C4}$$

To compute this quantity, let us introduce the complex function

$$g_{E,x}(\kappa) = \frac{e^{i|x|\kappa}}{\sqrt[4]{\kappa^2+m^2}(E-\sqrt{\kappa^2+m^2})}\pi\left[\cot\left(\frac{\kappa L}{2}\right) - i\right]. \tag{C5}$$

By the residue theorem,

$$\frac{1}{2\pi i}\oint_\Gamma g_{E,x}(\kappa)\,d\kappa$$

$$= \sum_{k=-\infty}^{\infty}\text{Res}_{g_{E,x}}\left(\frac{2\pi k}{L}\right) + \text{Res}_{g_{E,x}}(\sqrt{E^2-m^2})\theta(E)$$

$$+ \text{Res}_{g_{E,x}}(-\sqrt{E^2-m^2})\theta(E). \tag{C6}$$

The terms in the last equation are easily obtained:

$$\text{Res}_{g_{E,x}}\left(\frac{2\pi k}{L}\right) = \frac{2\pi}{L}\frac{1}{\sqrt{\omega_k}(E-\omega_k)}\exp\left(\frac{2\pi ik|x|}{L}\right), \tag{C7}$$

as well as

$$\text{Res}_{g_{E,x}}(\pm\sqrt{E^2-m^2}) = -e^{\pm i|x|\sqrt{E^2-m^2}}\sqrt{\frac{E}{E^2-m^2}}\pi\left[\cot\left(\frac{L\sqrt{E^2-m^2}}{2}\right)\mp i\right], \tag{C8}$$

finally yielding

$$\frac{2\pi}{L}\sum_{k=-\infty}^{\infty}\frac{1}{\sqrt{\omega_k}(\omega_k-E)}\exp\left(\frac{2\pi ik|x|}{L}\right) = 2\pi\sqrt{\frac{E}{E^2-m^2}}\left[\cot\left(\frac{L\sqrt{E^2-m^2}}{2}\right)\cos(x\sqrt{E^2-m^2})\right.$$
$$\left.+\sin(|x|\sqrt{E^2-m^2})\right]\theta(E) + \frac{1}{2\pi i}\oint_\Gamma g_{E,x}(\kappa)\,d\kappa. \tag{C9}$$

Choosing again a contour that encircles both branch cuts of $g_{E,x}(\kappa)$ as in Fig. 5, we get

$$\oint_\Gamma g_{E,x}(\kappa)\,d\kappa = \int_{im-0^+}^{i\infty-0^+} g_{E,x}(\kappa)\,d\kappa - \int_{im+0^+}^{i\infty+0^+} g_{E,x}(\kappa)\,d\kappa + \int_{-im+0^+}^{-i\infty+0^+} g_{E,x}(\kappa)\,d\kappa - \int_{-im-0^+}^{-i\infty-0^+} g_{E,x}(\kappa)\,d\kappa$$

$$= i\int_m^\infty (g_{E,x}(iy-0^+) - g_{E,x}(iy+0^+))\,dy - i\int_m^\infty (g_{E,x}(-iy+0^+) - g_{E,x}(-iy-0^+))\,dy$$

$$= -2\pi i\int_m^\infty \frac{e^{-|x|y}}{e^{-Ly}-1}\frac{\sqrt{2}(E-\sqrt{y^2-m^2})}{\sqrt[4]{y^2-m^2}(E^2+y^2-m^2)}\,dy + 2\pi i\int_m^\infty \frac{e^{|x|y}}{e^{Ly}-1}\frac{\sqrt{2}(E-\sqrt{y^2-m^2})}{\sqrt[4]{y^2-m^2}(E^2+y^2-m^2)}\,dy$$

$$= 2\sqrt{2}\pi i\int_m^\infty \frac{e^{-|x|y}+e^{-(L-|x|)y}}{1-e^{-Ly}}\frac{1}{\sqrt[4]{y^2-m^2}}\frac{E-\sqrt{y^2-m^2}}{E^2+y^2-m^2}\,dy$$

$$= 2\sqrt{2}\pi i\int_m^\infty \frac{\cosh(|x|y)\coth\left(\frac{Ly}{2}\right)-\sinh(|x|y)}{\sqrt[4]{y^2-m^2}}\frac{E-\sqrt{y^2-m^2}}{E^2+y^2-m^2}\,dy. \tag{C10}$$

We finally obtain

$$\xi_1(x) = \sqrt{\frac{2\pi\gamma E}{E^2-m^2}}\left[\cot\left(\frac{L\sqrt{E^2-m^2}}{2}\right)\cos(x\sqrt{E^2-m^2})+\sin(|x|\sqrt{E^2-m^2})\right]\theta(E) + \eta(x), \tag{C11}$$

where

$$\eta(x) = \sqrt{\frac{\gamma}{\pi}}\int_m^\infty \frac{\cosh(|x|y)\coth\left(\frac{Ly}{2}\right)-\sinh(|x|y)}{\sqrt{y^2-m^2}}\frac{E-\sqrt{y^2-m^2}}{E^2+y^2-m^2}\,dy, \tag{C12}$$

the latter term vanishing exponentially far from $x=0$. This completes the description of the eigensystem of the model. In particular, we can comment on the pair of resonant two-emitter states involved in the implementation of a qubit, discussed in Sec. IV. While in the case of weak coupling the emitters retain the largest part of the excitation, in the strong-coupling regime the photonic component becomes dominant. In both regimes, the emitter excitation for the symmetric state is larger than in the antisymmetric case.

[1] D. Roy, C. M. Wilson, and O. Firstenberg, *Colloquium*: Strongly interacting photons in one-dimensional continuum, Rev. Mod. Phys. **89**, 021001 (2017).

[2] E. Vetsch, D. Reitz, G. Sague, R. Schmidt, S. T. Dawkins, and A. Rauschenbeutel, Optical Interface Created by Laser-Cooled Atoms Trapped in the Evanescent Field Surrounding an Optical Nanofiber, Phys. Rev. Lett. **104**, 203603 (2010).

[3] M. Bajcsy, S. Hofferberth, V. Balic, T. Peyronel, M. Hafezi, A. S. Zibrov, V. Vuletic, and M. D. Lukin, Efficient All-Optical Switching Using Slow Light within a Hollow Fiber, Phys. Rev. Lett. **102**, 203902 (2009).

[4] U. Dorner and P. Zoller, Laser-driven atoms in half-cavities, Phys. Rev. A **66**, 023816 (2002).

[5] G. Zumofen, N. M. Mojarad, V. Sandoghdar, and M. Agio, Perfect Reflection of Light by an Oscillating Dipole, Phys. Rev. Lett. **101**, 180404 (2008).

[6] N. Lindlein, R. Maiwald, H. Konermann, M. Sondermann, U. Peschel, and G. Leuchs, A new 4π geometry optimized for focusing on an atom with a dipole-like radiation pattern, Laser Phys. **17**, 927 (2007).

[7] P. Lodahl, S. Mahmoodian, and S. Stobbe, Interfacing single photons and single quantum dots with photonic nanostructures, Rev. Mod. Phys. **87**, 347 (2015).

[8] A. Wallraff, D. I. Schuster, A. Blais, L. Frunzio, R.-S. Huang, J. Majer, S. Kumar, S. M. Girvin, and R. J. Schoelkopf, Strong coupling of a single photon to a superconducting qubit using

circuit quantum electrodynamics, Nature (London) **431**, 162 (2004).

[9] O. Astafiev, A. M. Zagoskin, A. A. Abdumalikov, Jr., Yu. A. Pashkin, T. Yamamoto, K. Inomata, Y. Nakamura, and J. S. Tsai, Resonance fluorescence of a single artificial atom, Science **327**, 840 (2010).

[10] I.-C. Hoi, A. F. Kockum, L. Tornberg, A. Pourkabirian, G. Johansson, P. Delsing, and C. M. Wilson, Probing the quantum vacuum with an artificial atom in front of a mirror, Nat. Phys. **11**, 1045 (2015).

[11] H. Dong, Z. R. Gong, H. Ian, L. Zhou, and C. P. Sun, Intrinsic cavity QED and emergent quasinormal modes for a single photon, Phys. Rev. A **79**, 063847 (2009).

[12] T. Tufarelli, F. Ciccarello, and M. S. Kim, Dynamics of spontaneous emission in a single-end photonic waveguide, Phys. Rev. A **87**, 013820 (2013).

[13] J.-T. Shen and S. Fan, Coherent Single Photon Transport in a One-Dimensional Waveguide Coupled with Superconducting Quantum Bits, Phys. Rev. Lett. **95**, 213001 (2005).

[14] A. Faraon, E. Waks, D. Englund, I. Fushman, and J. Vučković, Efficient photonic crystal cavity-waveguide couplers, Appl. Phys. Lett. **90**, 073102 (2007).

[15] B. Dayan, A. S. Parkins, T. Aoki, E. P. Ostby, K. J. Vahala, and H. J. Kimble, A photon turnstile dynamically regulated by one atom, Science **319**, 1062 (2008).

[16] J. S. Douglas, H. Habibian, C.-L. Hung, A. V. Gorshkov, H. J. Kimble, and D. E. Chang, Quantum many-body models with cold atoms coupled to photonic crystals, Nat. Photonics **9**, 326 (2015).

[17] A. Goban, C.-L. Hung, J. D. Hood, S.-P. Yu, J. A. Muniz, O. Painter, and H. J. Kimble, Superradiance for Atoms Trapped along a Photonic Crystal Waveguide, Phys. Rev. Lett. **115**, 063601 (2015).

[18] A. González-Tudela, V. Paulisch, H. J. Kimble, and J. I. Cirac, Efficient Multiphoton Generation in Waveguide Quantum Electrodynamics, Phys. Rev. Lett. **118**, 213601 (2017).

[19] J. Bleuse, J. Claudon, M. Creasey, N. S. Malik, J. M. Gerard, I. Maksymov, J. P. Hugonin, and P. Lalanne, Inhibition, Enhancement, and Control of Spontaneous Emission in Photonic Nanowires, Phys. Rev. Lett. **106**, 103601 (2011).

[20] M. E. Reimer, G. Bulgarini, N. Akopian, M. Hocevar, M. B. Bavinck, M. A. Verheijen, E. P. A. M. Bakkers, L. P. Kouwenhoven, and V. Zwiller, Bright single-photon sources in bottom-up tailored nanowires, Nat. Commun. **3**, 737 (2012).

[21] T. Shi, D. E. Chang, and J. I. Cirac, Multiphoton-scattering theory and generalized master equations, Phys. Rev. A **92**, 053834 (2015).

[22] T. Shi, Y.-H. Wu, A. Gonzalez-Tudela, and J. I. Cirac, Bound States in Boson Impurity Models, Phys. Rev. X **6**, 021027 (2016).

[23] E. Sanchez-Burillo, D. Zueco, L. Martin-Moreno, and J. J. Garcia-Ripoll, Dynamical signatures of bound states in waveguide QED, Phys. Rev. A **96**, 023831 (2017).

[24] F. Lombardo, F. Ciccarello, and G. M. Palma, Photon localization versus population trapping in a coupled-cavity array, Phys. Rev. A **89**, 053826 (2014).

[25] K. Lalumière, B. C. Sanders, A. F. van Loo, A. Fedorov, A. Wallraff, and A. Blais, Input-output theory for waveguide QED

[26] D. Witthaut and A. S. Sørensen, Photon scattering by a three-level emitter in a one-dimensional waveguide, New J. Phys. **12**, 043052 (2010).

[27] A. Gonzalez-Tudela, D. Martin-Cano, E. Moreno, L. Martin-Moreno, C. Tejedor, and F. J. Garcia-Vidal, Entanglement of Two Qubits Mediated by One-Dimensional Plasmonic Waveguides, Phys. Rev. Lett. **106**, 020501 (2011).

[28] E. Shahmoon and G. Kurizki, Nonradiative interaction and entanglement between distant atoms, Phys. Rev. A **87**, 033831 (2013).

[29] P. Facchi, M. S. Kim, S. Pascazio, F. V. Pepe, D. Pomarico, and T. Tufarelli, Bound states and entanglement generation in waveguide quantum electrodynamics, Phys. Rev. A **94**, 043839 (2016).

[30] P. Facchi, S. Pascazio, F. V. Pepe, and K. Yuasa, Long-lived entanglement of two multilevel atoms in a waveguide, J. Phys. Commun. **2**, 035006 (2018).

[31] X. H. H. Zhang and H. U. Baranger, Heralded Bell State of 1D Dissipative Qubits Using Classical Light, Phys. Rev. Lett. **122**, 140502 (2019).

[32] H. Zheng and H. U. Baranger, Persistent Quantum Beats and Long-Distance Entanglement from Waveguide-Mediated Interactions, Phys. Rev. Lett. **110**, 113601 (2013).

[33] C. Gonzalez-Ballestero, F. J. Garcia-Vidal, and E. Moreno, Non-Markovian effects in waveguide-mediated entanglement, New J. Phys. **15**, 073015 (2013).

[34] E. S. Redchenko and V. I. Yudson, Decay of metastable excited states of two qubits in a waveguide, Phys. Rev. A **90**, 063829 (2014).

[35] M. Laakso and M. Pletyukhov, Scattering of Two Photons from Two Distant Qubits: Exact Solution, Phys. Rev. Lett. **113**, 183601 (2014).

[36] H. Pichler, T. Ramos, A. J. Daley, and P. Zoller, Quantum optics of chiral spin networks, Phys. Rev. A **91**, 042116 (2015).

[37] A. F. van Loo, A. Fedorov, K. Lalumière, B. C. Sanders, A. Blais, and A. Wallraff, Photon-mediated interactions between distant artificial atoms, Science **342**, 1494 (2013).

[38] A. Rosario Hamann, C. Müller, M. Jerger, M. Zanner, J. Combes, M. Pletyukhov, M. Weides, T. M. Stace, and A. Fedorov, Nonreciprocity Realized with Quantum Nonlinearity, Phys. Rev. Lett. **121**, 123601 (2018).

[39] G. Calajò, Y.-L. L. Fang, H. U. Baranger, and F. Ciccarello, Exciting a Bound State in the Continuum through Multiphoton Scattering Plus Delayed Quantum Feedback, Phys. Rev. Lett. **122**, 073601 (2019).

[40] P. Facchi, S. Pascazio, F. V. Pepe, and D. Pomarico, Correlated photon emission by two excited atoms in a waveguide, Phys. Rev. A **98**, 063823 (2018).

[41] K. Sinha, A. González-Tudela, Y. Lu, and P. Solano, Collective radiation from distant emitters, Phys. Rev. A **102**, 043718 (2020).

[42] V. I. Yudson, Dynamics of the integrable one-dimensional system "photons + two-level atoms", Phys. Lett. A **129**, 17 (1988).

[43] H. Pichler and P. Zoller, Photonic Circuits with Time Delays and Quantum Feedback, Phys. Rev. Lett. **116**, 093601 (2016).

[44] V. I. Yudson and P. Reineker, Multiphoton scattering in a one-dimensional waveguide with resonant atoms, Phys. Rev. A **78**, 052713 (2008).

[45] Y.-L. L. Fang and H. U. Baranger, Waveguide QED: Power spectra and correlations of two photons scattered off multiple distant qubits and a mirror, Phys. Rev. A **91**, 053845 (2015).

[46] T. S. Tsoi and C. K. Law, Quantum interference effects of a single photon interacting with an atomic chain inside a one-dimensional waveguide, Phys. Rev. A **78**, 063832 (2008).

[47] T. Ramos, B. Vermersch, P. Hauke, H. Pichler, and P. Zoller, Non-Markovian dynamics in chiral quantum networks with spins and photons, Phys. Rev. A **93**, 062104 (2016).

[48] M. Bello, G. Platero, J. I. Cirac, and A. González-Tudela, Unconventional quantum optics in topological waveguide QED, Sci. Adv. **5**, eaaw0297 (2019).

[49] H. Bernien, S. Schwartz, A. Keesling, H. Levine, A. Omran, H. Pichler, S. Choi, A. S. Zibrov, M. Endres, M. Greiner, V. Vuletić, and M. D. Lukin, Probing many-body dynamics on a 51-atom quantum simulator, Nature (London) **551**, 579 (2017).

[50] Y. Dong, Y.-S. Lee, and K. S. Choi, Waveguide QED toolboxes for synthetic quantum matter with neutral atoms, arXiv:1712.02020.

[51] Y. Fang, H. Zheng, and H. Baranger, One-dimensional waveguide coupled to multiple qubits: Photon-photon correlations, EPJ Quantum Technol. **1**, 3 (2014).

[52] X. Gu, A. F. Kockum, A. Miranowicz, Y.-X. Liu, and F. Nori, Microwave photonics with superconducting quantum circuits, Phys. Rep. **718-719**, 1 (2017).

[53] P. O. Guimond, H. Pichler, A. Rauschenbeutel, and P. Zoller, Chiral quantum optics with V-level atoms and coherent quantum feedback, Phys. Rev. A **94**, 033829 (2016).

[54] P. Lodahl, S. Mahmoodian, S. Stobbe, A. Rauschenbeutel, P. Schneeweiss, and J. Volz, Chiral quantum optics, Nature (London) **541**, 473 (2017).

[55] V. Paulisch, H. Kimble, and A. González-Tudela, Universal quantum computation in waveguide QED using decoherence free subspaces, New J. Phys. **18**, 043041 (2016).

[56] T. Ramos, H. Pichler, A. J. Daley, and P. Zoller, Quantum Spin Dimers from Chiral Dissipation in Cold-Atom Chains, Phys. Rev. Lett. **113**, 237203 (2014).

[57] G. Calajò, F. Ciccarello, D. Chang, and P. Rabl, Atom-field dressed states in slow-light waveguide QED, Phys. Rev. A **93**, 033833 (2016).

[58] A. F. Kockum, G. Johansson, and F. Nori, Decoherence-Free Interaction between Giant Atoms in Waveguide Quantum Electrodynamics, Phys. Rev. Lett. **120**, 140404 (2018).

[59] F. Dinc, A. M. Brańczyk, and I. Ercan, Real-space time dynamics in waveguide QED: Bound states and single-photon-pulse scattering, Quantum **3**, 213 (2019).

[60] P. Facchi, D. Lonigro, S. Pascazio, F. V. Pepe, and D. Pomarico, Bound states in the continuum for an array of quantum emitters, Phys. Rev. A **100**, 023834 (2019).

[61] Y. Zhou, Z. Chen, and J.-T. Shen, Single-photon superradiant emission rate scaling for atoms trapped in a photonic waveguide, Phys. Rev. A **95**, 043832 (2017).

[62] R. H. Dicke, Coherence in spontaneous radiation processes, Phys. Rev. **93**, 99 (1954).

[63] M. Gross and S. Haroche, Superradiance: An essay on the theory of collective spontaneous emission, Phys. Rep. **93**, 301 (1982).

[64] M. O. Araújo, I. Krešić, R. Kaiser, and W. Guerin, Superradiance in a Large and Dilute Cloud of Cold Atoms in the Linear-Optics Regime, Phys. Rev. Lett. **117**, 073002 (2016).

[65] N. Cherroret, M. Hemmerling, V. Nador, J. T. M. Walraven, and R. Kaiser, Robust Coherent Transport of Light in Multilevel Hot Atomic Vapors, Phys. Rev. Lett. **122**, 183203 (2019).

[66] L. Stern, B. Desiatov, I. Goykhman, and U. Levy, Nanoscale light–matter interactions in atomic cladding waveguides, Nat. Commun. **4**, 1548 (2013).

[67] L. Stern and U. Levy, Transmission and time delay properties of an integrated system consisting of atomic vapor cladding on top of a micro ring resonator, Opt. Express **20**, 28082 (2012).

[68] Y. Zhou, Z. Chen, and J.-T. Shen, Single-photon superradiance in waveguide-quantum-electrodynamical systems with whispering-gallery-mode resonators, Phys. Rev. A **101**, 043831 (2020).

[69] J. D. Jackson, *Classical Electrodynamics*, 3rd ed. (Wiley, Danvers, 1998).

[70] C. Cohen-Tannoudji, J. Dupont-Roc, and G. Grynberg, *Atom-Photon Interactions: Basic Processes and Applications* (Wiley-VCH Verlag, Weinheim, 1998).

[71] C. W. Hsu, B. Zhen, A. D. Stone, J. D. Joannopoulos, and M. Soljačić, Bound states in the continuum, Nat. Rev. Mater. **1**, 16048 (2016).

[72] K. Vahala, Optical microcavities, Nature (London) **424**, 839 (2003).

[73] A. D. Greentree, J. Salzman, S. Prawer, and L. C. L. Hollenberg, Quantum gate for Q switching in monolithic photonic-band-gap cavities containing two-level atoms, Phys. Rev. A **73**, 013818 (2006).

[74] R. Schoelkopf and S. Girvin, Wiring up quantum systems, Nature (London) **451**, 664 (2008).

[75] J. M. Gambetta, J. M. Chow, and M. Steffen, Building logical qubits in a superconducting quantum computing system, npj Quantum Inf. **3**, 2 (2017).

[76] P. Longo, P. Schmitteckert, and K. Busch, Few-Photon Transport in Low-Dimensional Systems: Interaction-Induced Radiation Trapping, Phys. Rev. Lett. **104**, 023602 (2010).

[77] E. Sánchez-Burillo, A. González-Tudela, and C. Gonzalez-Ballestero, Theory of waveguide-QED with moving emitters, Phys. Rev. A **102**, 013726 (2020).

[78] M. Aigner and G. M. Ziegler, *Proofs from THE BOOK*, 4th ed. (Springer-Verlag, Berlin, 2013).